

# Towards antiferromagnetic metal spintronics

J. Basset<sup>1,2</sup>, A. Sharma<sup>3</sup>, Z. Wei<sup>1</sup>, J. Bass<sup>3</sup>, and M. Tsoi<sup>1</sup>

<sup>1</sup>University of Texas at Austin, Austin, TX, USA

<sup>2</sup>University Joseph Fourier, Grenoble, France

<sup>3</sup>Michigan State University, East Lansing, MI, USA

## ABSTRACT

Spintronics is about control and manipulation of magnetic moments for new and improved functionality in electronic devices. The phenomenon of spin transfer emerged as a unique tool to control the magnetic state of a ferromagnet (F) with an electrical current. MacDonald and co-workers predicted that spin transfer could also occur in an antiferromagnet (AFM), where it might be even stronger under certain conditions. We recently showed that the exchange bias at an AFM/F interface, with AFM = FeMn and F = CoFe, could be either increased or decreased depending upon the polarity of the applied current. We attributed these changes to effects of the current on the AFM. Here we extend that study to a new AFM = IrMn and to a new F = Py = Ni<sub>x</sub>Fe<sub>1-x</sub> with  $x \sim 0.2$ . Using exchange-biased spin-valves (EBSVs) of the form AFM/F(pinned)/Cu/F(free), where both Fs are the same alloy, we first compare data for F = CoFe with AFMs = FeMn or IrMn. The data for FeMn and IrMn are generally similar, with the current having clear effects upon the exchange bias, but little or none on the coercive field of the ‘free’ CoFe-layer. We then present data for F = Py with AFMs = FeMn or IrMn. With Py, the current generally affects both the exchange bias and the coercive field of the ‘free’ layer, in ways that we are not yet able to simply correlate with layer thicknesses or AFM.

**Keywords:** spin-transfer torque, exchange bias, multilayer, spin valve, giant magnetoresistance

## 1. INTRODUCTION

Spintronics in ferromagnetic systems is built on a complementary set of phenomena in which the magnetic configuration of the system influences its transport properties and vice versa. Giant magnetoresistance (GMR)<sup>1, 2</sup> and spin transfer torque<sup>3-5</sup> exemplify such interconnections in multilayers composed of ferromagnetic (F) and non-magnetic (N) layers. Recently, MacDonald and co-workers<sup>6</sup> predicted that corresponding effects ought to occur in multilayers where the F components are replaced by AFMs. First, they predicted that the resistance of an AFM spin valve – where two AFM layers are separated by an N spacer – could depend upon the relative orientations of the magnetic moments in the two AFM layers (antiferromagnetic GMR = AGMR). Second, they predicted that injecting a strong enough current density into an AFM should affect its magnetic state via current-induced spin torque. According to Ref. 6, the critical current needed to alter the magnetic order in AFMs can be smaller than for Fs, due to the absence of shape anisotropy and because spin torques can act through the entire AFM volume. These new AFM effects could potentially lead to new all-AFM spintronics where AFMs are used in place of Fs. However, the calculations are all for perfect samples and depend upon quantum coherence. It is known that disorder can reduce the predicted effects. Experiments are thus crucial to see if any such effects are visible in real samples.

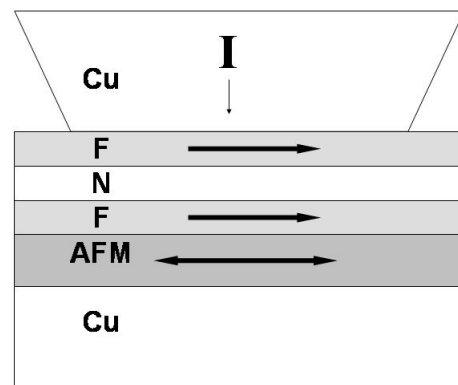
We<sup>7</sup> and Urazhdin and Anthony<sup>8</sup> in the Current-Perpendicular-to-Plane (CPP) geometry, and others in the Current-In-Plane (CIP) geometry<sup>9, 10</sup> recently published studies of effects of high current densities on exchange bias at an AFM/F interface. These studies were reviewed in Ref. 11. In our original experiments<sup>7</sup> we showed that the strength of the exchange bias<sup>12-14</sup> at an AFM/F = FeMn/CoFe interface (FeMn = Fe<sub>1-x</sub>Mn<sub>x</sub> with  $x \sim 0.5$  and CoFe = Co<sub>1-x</sub>Fe<sub>x</sub> with  $x \sim 0.09$ ) could be increased or decreased (up to 30%) by an electric current flowing approximately perpendicular to the interface. As exchange bias is known to be associated with interfacial AFM magnetic moments,<sup>15-17</sup> our observation<sup>7</sup> can be taken as the first evidence of effects of the current on the AFM predicted in Ref. 6. However, the data do not

distinguish effects of the current on bulk or interfacial AFM moments. In hopes of clarifying the situation, we have extended that study to a new AFM = IrMn = Ir<sub>x</sub>Mn<sub>1-x</sub> with x = 0.2 and to a new F = Permalloy (Py = Ni<sub>1-x</sub>Fe<sub>x</sub> with x ~ 0.2). This paper, describing some of these new results, is organized as follows: We first briefly review our experimental technique and original findings with exchange-biased spin-valves (EBSVs) of the form AFM/F(pinned)/Cu/F(free) and the AFM = FeMn and the F = CoFe. We then compare these results with new ones for F = CoFe but the AFM = IrMn. The data for FeMn and IrMn are generally similar, with the current having clear and similar effects upon the exchange bias, but little or no effect on the coercive field of the ‘free’ CoFe-layer. Finally we extend our study to F = Py with AFMs = FeMn or IrMn. With Py, the current usually affects both the exchange bias and the coercive field of the ‘free’ layer, but the variations are not always simple and we have not yet been able to correlate them in a simple way with layer thicknesses.

## 2. EXPERIMENTAL INFORMATION

As illustrated in Fig. 1, we use a point-contact (~ 10-100 nm in diameter) to inject a current density up to ~10<sup>12</sup> A/m<sup>2</sup> approximately perpendicular (CPP) to the layers of an exchange-biased spin valve (EBSV), and measure R(B), the resistance as a function of magnetic field B, for different fixed values of positive and negative current +I and -I. Each EBSV contains two F layers separated by a nonmagnetic (N) spacer, with one F-layer exchange biased by an adjacent AFM. The AFM/F(pinned)/Cu/F(free) spin-valves are sputtered onto Si substrates using techniques described elsewhere<sup>18</sup>. Prior to measurements the samples are exchange-biased by heating to ~453 K (for FeMn) or ~527K (for IrMn), above the blocking temperatures of the AFMs, and then cooled in a magnetic field ~180 Oe. The N = Cu spacer layer is 10 nm thick to eliminate exchange coupling between the two F-layers. The top layer is covered by a 5 nm thick Au layer to protect it from atmospheric contamination. The sharpened Cu tip that makes the contact is moved towards the EBSV using a standard differential screw mechanism.<sup>5</sup> All EBSVs have a thick (50 or 100 nm) Cu underlayer to secure a closely CPP current flow from the point contact, across the spin valve, and into the Cu buffer. The density j of the current is defined by the contact size (resistance)<sup>5</sup> and the magnitude of I; a typical contact resistance of 1-2 Ω and I = 10 mA corresponds to ~ 10<sup>12</sup> A/m<sup>2</sup>.

**Fig. 1.** Sample schematic shown with the magnetizations of the two ferromagnetic (F) layers oriented in the parallel (P) state. A sharpened Cu tip makes a point contact with an extended exchange-biased spin-valve (EBSV). Omitted from the picture is a 5 nm thick Au protective layer between the Cu tip and the top ‘free’ F-layer. The bottom F-layer is exchange-bias pinned to the adjacent antiferromagnetic (AFM) layer as described in the text. In the text, the layer thicknesses are specified in nm. The bottom Cu layer is 50-100 nm thick.

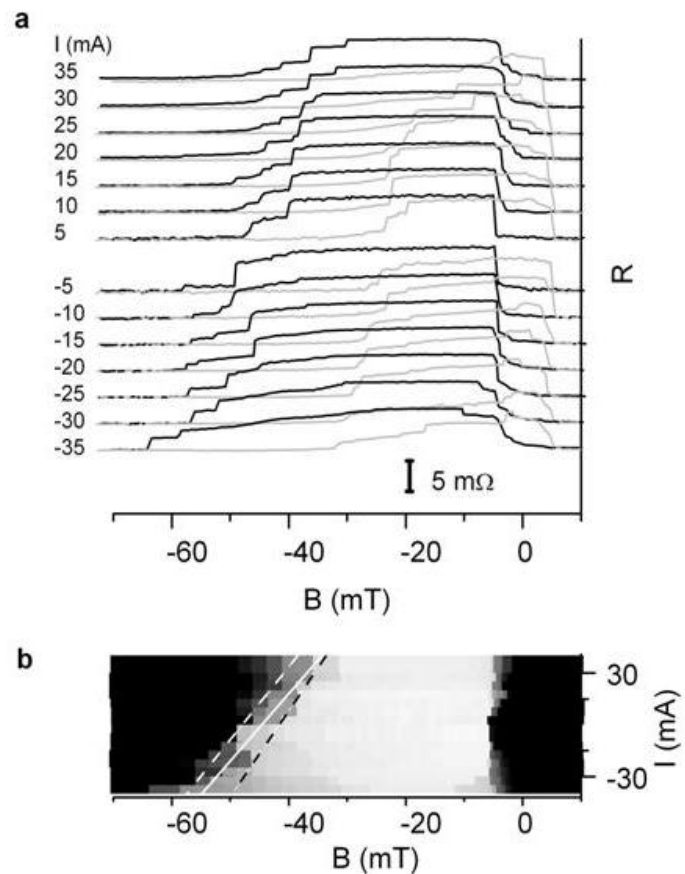


## 3. DATA FOR F = CoFe AND AFM = FeMn

We first briefly review results obtained for FeMn/CoFe/Cu/CoFe EBSVs (the specified order for the EBSVs in figures is from the thick Cu bottom layer up to the point contact) by Wei et al.<sup>7</sup> Figure 2a shows R(B) hysteresis traces for different applied currents for an FeMn(8)/CoFe(3)/Cu(10)/CoFe(10) sample. Here, and hereafter, layer thicknesses are given in nm. Figure 2b shows the down magnetic field-sweeps (i.e., from large + B to large -B) of Fig. 2a in 2D gray-scale plot representation, where lighter color indicates higher resistance [white = antiparallel (AP) state and black =

parallel (P) state]. The coercive field of the 'free' CoFe layer is almost independent of the applied current. In contrast, the current both broadens the reversal of the pinned CoFe, and on average increases the exchange-bias with applied negative current (-I) and decreases it with positive current (+I). These shifts in bias are opposite to what is expected for standard spin transfer between the free and pinned F layers, which should increase the reversal field of the pinned F (stabilize the P configuration of the F layers) at positive bias and decrease it at negative bias. In contrast, the observed behavior agrees qualitatively with the predictions by Nunez et al.<sup>6</sup> for AFM spin transfer. To quantify the shifts, the white dashed, white solid, and black-dashed lines in Fig. 2b show least-squares linear fits to the R(B) data points at the 30%, 50%, and 70% levels, respectively, assuming 0% for minimum resistance (P state) and 100% for maximum resistance (AP state). The resulting slopes of 0.23 (30%), 0.26 (50%), and 0.2 (70%) T/A both emphasize the overall trend and highlight stochastic variations on top of this trend, as well as differential effects of broadening on the different linear fits. The absence of any effect of current on the free CoFe layer suggests that, for FeMn and CoFe, regular spin-transfer interactions between the two CoFe layers are significantly weaker than this new effect at the FeMn/CoFe interface. Similar behaviors were observed for a free layer thickness of 3 nm<sup>7</sup>, showing that they were not sensitive to the thickness of the 'free' CoFe-layer.

**Fig. 2.** (a) 3 dimensional (3D) representation of resistance R(B) hysteresis curves vs magnetic field B, for various currents I, for an 0.92 Ω point contact to a FeMn(8)/CoFe(3)/Cu(10)/CoFe(10) EBSV. The vertical scale size of 5 mΩ is indicated. The solid curves are 'down' sweeps (from large +B to large -B). The grey curves are 'up' sweeps (from large -B to large +B). (b) 2D grey scale plot of the 'down'-sweep R(B) data of Fig. 2a, with white = maximum R (AP state) and black = minimum R (P state). The dashed white (30%), solid white (50%) and dashed black (70%) lines represent linear fits to the data at the indicated percentage of full scale [100% = R(AP) - R(P)]. (After ref. [7]).



#### 4. DATA FOR F = CoFe AND AFM = IrMn

We next present results for IrMn/CoFe/Cu/CoFe EBSVs. IrMn is the AFM of choice for the magnetic recording industry due to its good combination of magnetic, thermal and corrosion properties. To compare the behavior for this new AFM with that we saw with FeMn, we focus here on an IrMn(8)/CoFe(3)/Cu(10)/CoFe(10) EBSV with the same thicknesses of F, N, and AFM layers as for FeMn in Fig. 2. Figures 3a and 3b show up and down R(B) field-sweeps, respectively, in 2D gray-scale plot representation for a 2 Ohm contact to this EBSV. As with FeMn, the reversal of the free CoFe(10) layer is not affected by the applied current. Also as with FeMn, for the up sweep the reversal of the pinned

layer shifts on average towards lower/higher magnitude fields for higher positive/negative applied currents. The down sweep behavior is more equivocal. Figures 4a (up-sweep) and 4b (down-sweep) show similar results for an inverted version [i.e., CoFe(10)/Cu(10)/CoFe(3)/IrMn(8)] of the same EBSV. Again the applied current affects only the pinned layer. And, as with FeMn<sup>7</sup>, the directions of shifts of reversal of the pinned layer are opposite to those in Fig. 3, now shifting on average, towards higher/lower magnitude fields for higher positive/negative currents. We conclude that the data for AFM = IrMn are generally similar to those previously seen with AFM = FeMn, with the current having similar effects upon the exchange bias, but little or no effect upon the coercive field of the ‘free’ CoFe-layer. The least-squares linear fits to the R(B) data points at the 30%, 50%, and 70% levels, respectively, give 0.7/-0.07 (30%), 0.64/-0.78 (50%), and 0.63/0.59 (70%) T/A slopes for the exchange bias vs current dependencies in Figs. 3a/4a. As noted for Fig. 2, the variations in slopes between the dashed white, solid white, and dashed black lines reflect both stochastic variations in the data and differential effects of broadening of the hysteresis curves upon the linear fits.

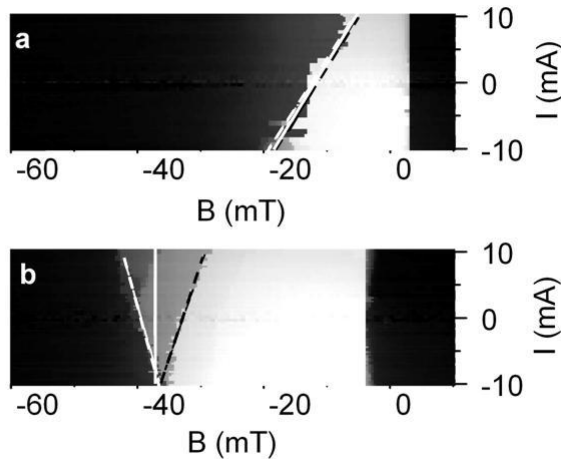


**Fig. 3.** 2D grey scale plots of R(B) hysteresis data vs I for a 2 Ω point contact to a IrMn(8)/ CoFe(3)/ Cu(10)/ CoFe(10) EBSV. The dashed white (30%), solid white (50%), and dashed black (70%) lines represent linear fits to the data at the indicated percentage of full scale as in Fig. 2b. (a) ‘up’ sweep. (b) ‘down’ sweep, as defined in Fig. 2a.

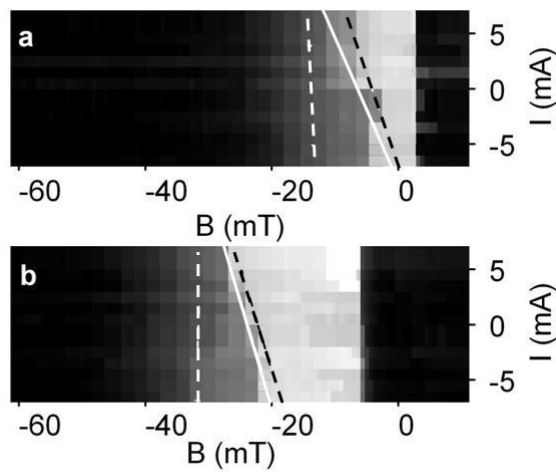


**Fig. 4.** 2D grey scale plots of R(B) hysteresis data vs I for a 2.75 Ω point contact to an inverted version of the sample of Fig. 3: CoFe(10)/ Cu(10)/ CoFe(3)/ IrMn(8) EBSV. The dashed white (30%), solid white (50%), and dashed black (70%) lines represent linear fits to the data at the indicated percentage of full scale as in Fig. 2b. (a) ‘up’ sweep. (b) ‘down’ sweep, as defined in Fig. 2a.

### 5. DATA FOR F = Py WITH BOTH AFM = FeMn AND IrMn

So far we have described the R(B) response to high current densities in AFM/F/N/F EBSVs with two different AFM materials (FeMn and IrMn) but always the same F = CoFe. In this section we describe some of what we found in EBSVs with F = Py.

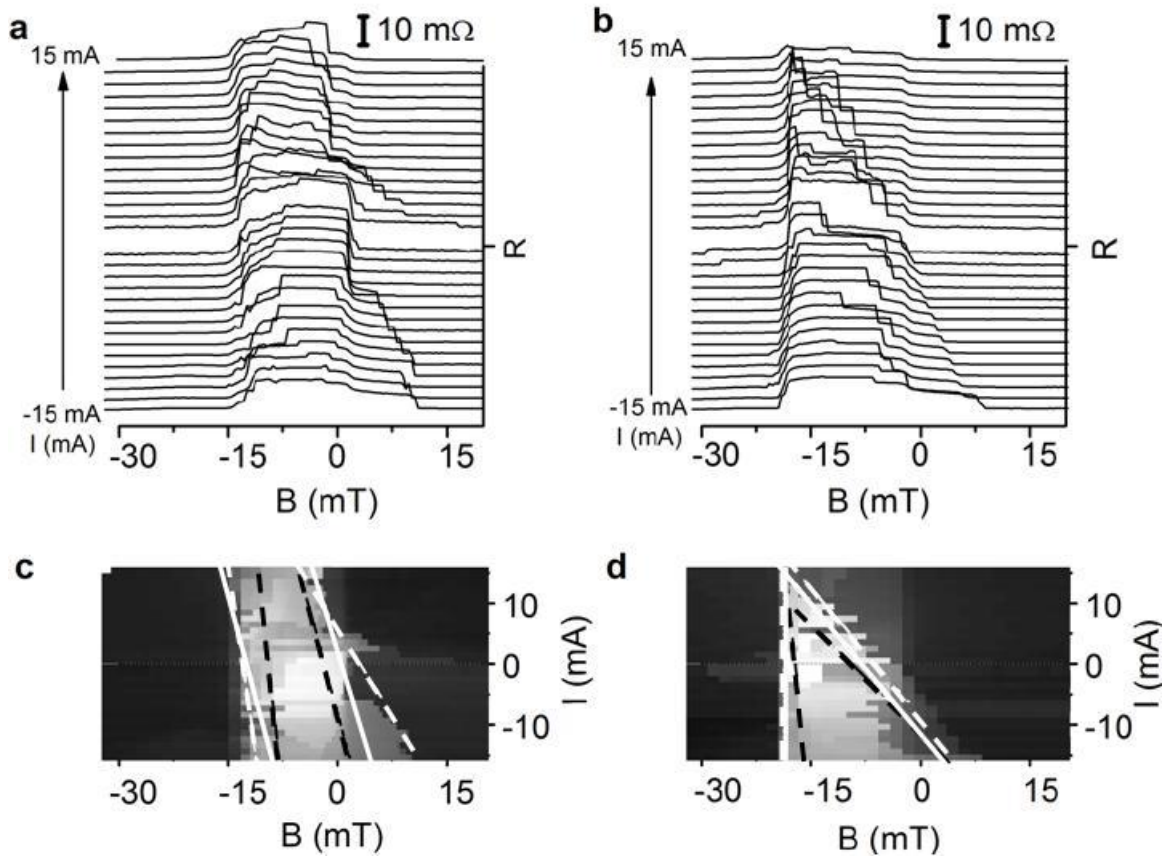


**Fig. 5.** (a, b) 3 dimensional (3D) representation of resistance  $R(B)$  hysteresis curves for various applied currents  $I$ , for a  $1.5 \Omega$  point contact to a FeMn(8)/Py(10)/Cu(10)/Py(3) EBSV. The vertical scale size of  $10 \text{ m}\Omega$  is indicated. Curve (b) is a 'down' sweep (from large +B to large -B). Curve (a) is an 'up' sweep (from large -B to large +B). (c, d) 2D grey scale plots of the  $R$  data of Fig. 5a, b with white = maximum  $R$  (AP state) and black = minimum  $R$  (P state). The dashed white (30%), solid white (50%) and dashed black (70%) lines represent linear fits to the data at the indicated percentage of full scale (100% =  $R(\text{AP}) - R(\text{P})$ ). Curve (c) is for the 'up' sweep; curve (d) is for the 'down' sweep.

With Py, we usually find the current to affect both the exchange-bias field of the 'pinned' F layer and the coercive field of the 'free' F layer. However, the behaviors are not the same for samples with AFM = FeMn or IrMn, nor for samples with the same AFM but different thicknesses of the 'free' and 'pinned' F layers. In this paper we focus on data for fixed pinned Py thickness of 10 nm. We present data for contacts to: (i) a FeMn(8)/Py(10)/Cu(10)/Py(3) spin-valve sample with a 3 nm thick 'free' Py layer; (ii) a FeMn(8)/Py(10)/Cu(10)/Py(10) spin valve with a 10 nm thick free Py layer; and (iii) an IrMn(8)/Py(10)/Cu(10)/Py(10) sample with equal Py-layer thicknesses but AFM = IrMn. The data shown are representative of those found for different contact resistances to the same samples.

- (i) For an FeMn(8)/Py(10)/Cu(10)/Py(3) EBSV, Fig. 5 shows both  $R(B)$  hysteresis curves (a and b) and 2D grey-scale plots (c and d). Graphs a and c are for  $B$  swept 'up' from large -  $B$  to large + $B$ ; graphs b and d are for  $B$  swept 'down'. Contrary to what we saw with CoFe, in all four graphs, the current has relatively little effect on the pinned layer, but larger effect on the 'free' layer. In b and d, + $I$  moves the 30%, 50%, and 70% lines for the free Py layer toward more negative field and - $I$  moves it to more positive field. But - $I$  also broadens the transition in a way that complicates the picture. Graphs a and c show similar, but less dramatic, changes for the free layer, again complicated somewhat by broadening for - $I$ .
- (ii) An FeMn(8)/Py(10)/Cu(10)/Py(10) EBSV gives a completely different behavior of  $R(B)$  as a function of  $I$ , as illustrated in 2D grey scale plots in Fig. 6. The applied current  $I$  now affects reversals of both the 'free' and

'pinned' layers, but the effect looks to be roughly symmetrical in  $I$ . White lines in Fig. 6 indicate now only the 50% least-squares linear fits taken independently for pinned and free Py layers for + $I$  and - $I$ .

- (iii) An IrMn(8)/Py(10)/Cu(10)/Py(10) spin valve gives still different behavior, as illustrated in an  $R(B)$  2D grey-scale plot in Fig. 7. Now, the free layer is unaffected by - $I$ , but + $I$  moves the reversal to more negative fields. In contrast, the pinned layer is unaffected by + $I$ , but - $I$  moves the reversal to smaller negative fields. Again white lines show only the 50% least-squares linear fits taken independently for pinned and free Py layers for + $I$  and - $I$ .

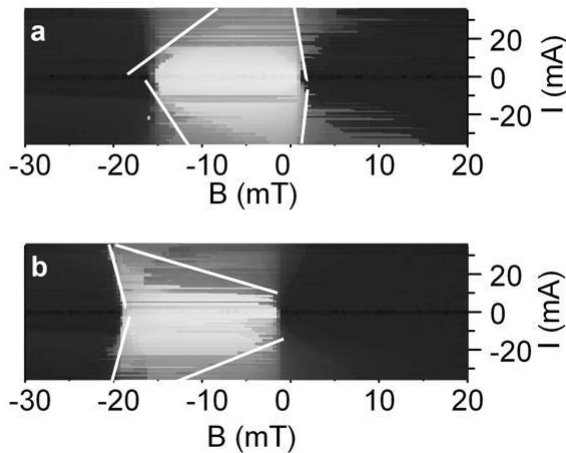


**Fig. 6.** 2D grey scale plots of  $R(B)$  hysteresis data vs  $I$ , for a  $2.76 \Omega$  point contact to a FeMn(8)/ Py(10)/ Cu(10)/ Py(10) EBSV. The solid white lines represent linear fits to the data at 50% of full scale taken independently for + $I$  and - $I$ . **(a)** 'up' sweep. **(b)** 'down' sweep, as defined in Fig. 2a.

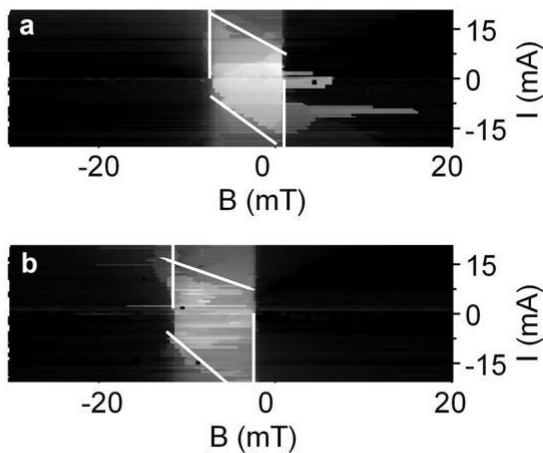


**Fig. 7.** 2D grey scale plots of  $R(B)$  hysteresis data vs  $I$ , for a  $2.5 \Omega$  point contact to an IrMn(8)/ Py(10)/ Cu(10)/ Py(10) EBSV. The solid white lines represent linear fits at 50% of full scale taken independently for + $I$  and - $I$ . **(a)** 'up' sweep. **(b)** 'down' sweep, as defined in Fig. 2a.

## 6. DISCUSSION

Since all of the IrMn/CoFe/N/CoFe data look rather similar to all of the FeMn/CoFe/N/CoFe data, and both sets of data are insensitive to whether the 'free' CoFe-layer was 3 nm or 10 nm thick, we can explain the behaviors of the IrMn data using the same qualitative model as in Ref. 7. It was assumed in Ref. 7 that the spin-transfer torque (STT) on the 'free' CoFe was not large enough to perturb its reversals, and it was argued that the shifts in exchange bias at the FeMn/CoFe interface could be understood as effects of STT acting on the bulk of the FeMn,<sup>7</sup> with information then transferred to the interface.

Because the AFM/Py/Cu/Py data neither behave like the AFM/CoFe/Cu/CoFe data, nor behave similarly for AFM=FeMn and AFM=IrMn, and are not independent of the ‘free’ Py layer thickness, it is clear that the simple assumptions used to explain AFM/CoFe/Cu/CoFe are insufficient. The presence of effects with Py on both the ‘pinned’ and ‘free’ F-layers suggests that, unlike AFM/CoFe/Cu/CoFe, the AFM/Py/Cu/Py samples may involve strong enough STT interactions between the two F layers to affect reversals of both. The lack of easily systematized behaviors in the three samples with Py that we presented, also portends the need for a more complex explanation. In particular, the linear behaviors that we've assumed for analyses may be too simple, with data on more samples likely to lead to changes in the analysis assumptions. For these reasons, we feel it appropriate to be cautious in trying to interpret in any simple way the full range of data in Figs. 2-7. We, thus, end this section by simply describing some potential contributions that will have to be considered in interpreting more complete data.

- (1) Mutual effects of STT acting on both F-layers – the ‘pinned’ and ‘free’ layers. As noted above, these STT effects alone should tend to induce opposite changes in the reversal of the ‘pinned’ F to those seen with CoFe. From the perspective of the Slonczewski and subsequent diffusive theories of spin-torque, Py and CoFe have generally similar transport parameters.<sup>19,20</sup> So we'd expect the STTs themselves to be similar for given layer thicknesses of CoFe and Py. However, CoFe and Py have magnetic differences, such as Py's much smaller values of both coercivity and magnetocrystalline anisotropy, which can affect the reversal process.
- (2) STT acting on the AFM layers, which were proposed in Ref. 7 to explain the observed (assumed linear) variations in exchange-bias of the ‘pinned’ layer. To first approximation, we'd expect such STT to be independent of the F-metal. However its effects could differ due to potential differences in domain structures in either the AFM, F, or both. Also, for an IrMn/Py interface, the majority metals on both sides are Mn and Ni. Intermixing of Mn and Ni across the interface could add still another AFM (i.e., NiMn) to the mix, further complicating the problem. Such effects can also not be completely ruled out with FeMn, where the Mn is 50%.
- (3) Heating effects due to the large values of the injected  $I_s$ . Such effects might be the source (or at least one of the sources) of the broadening seen in several of the figures above.
- (4) The response of different ‘free’ F-layers could also be affected by formation of different magnetic domain structures and different domain sizes in both the F- and AFM-layers, as well as by different abilities of domain walls to move under the action of STT.

## 7. SUMMARY AND CONCLUSIONS

Following predictions that strong current densities could produce spin-transfer-torque (STT)-like effects on antiferromagnets (AFMs)<sup>6, 21, 22</sup> we made an attempt to observe such effects in exchange-biased spin valves (EBSVs). Our original observation<sup>7</sup> of the current-dependent exchange bias at a FeMn/CoFe interface was proposed as the first evidence of effects of the current on the AFM. We now confirmed those observations with a new AFM material – IrMn. We also started to extend our studies to a new F = Py. With Py, we sometimes see, for the first time, the effect of current on both the AFM/F and the ‘free’ F components of the EBSVs. Unfortunately, the totality of the data now available show a variety of apparently different behaviors that make it difficult to decide precisely which physical phenomena are present. We are, thus, limited to suggesting several possibilities that will have to be examined via more complete data sets, and concluding that further studies are still needed to elucidate the dependence of these spin-transfer effects on metal combinations and layer thicknesses.

## ACKNOWLEDGMENTS

We are grateful to A. H. MacDonald, R. A. Duine, P. M. Haney, and A. S. Nunez for many insightful discussions. This work was supported in part by NSF grants DMR-06-45377 and DMR-08- 04126.

## REFERENCES

- [1] Baibich, M. N. et al., "Giant magnetoresistance of (001) Fe/(001) Cr magnetic superlattices," *Phys. Rev. Lett.* 61, 2472-2475 (1988).
- [2] Binasch, G., Grünberg, P., Saurenbach, F., Zinn, W., "Enhanced magnetoresistance in layered magnetic structures with antiferromagnetic interlayer exchange," *Phys. Rev. B* 39, 4828-4830 (1989).
- [3] Slonczewski, J. C., "Current-driven excitation of magnetic multilayers," *J. Magn. Magn. Mater.* 159, L1-L7 (1996).
- [4] Berger, L., "Emission of spin waves by a magnetic multilayer traversed by a current," *Phys. Rev. B* 54, 9353-9358 (1996).
- [5] Tsoi, M. et al., "Excitation of a magnetic multilayer by an electric current," *Phys. Rev. Lett.* 80, 4281-4284 (1998).
- [6] Núñez, A. S., Duine, R. A., Haney, P., MacDonald, A. H., "Theory of spin torques and giant magnetoresistance in antiferromagnetic metals," *Phys. Rev. B* 73, 214426 (2006).
- [7] Wei, Z. et al., "Changing exchange bias in spin valves with an electric current," *Phys. Rev. Lett.* 98, 116603 (2007).
- [8] Urazhdin, S., Anthony, N., "Effect of polarized current on the magnetic state of an antiferromagnet," *Phys. Rev. Lett.* 99, 046602 (2007).
- [9] Tang, X-L., et al., "Changing and reversing the exchange bias in a current-in-plane spin valve by means of an electric current," *Appl. Phys. Lett.* 91, 122504 (2007).
- [10] Dai, N.V., et al., "Impact of in-plane currents on magnetoresistance properties of an exchange-biased spin valve with an insulating antiferromagnetic layer," *Phys. Rev. B* 77, 132406 (2008).
- [11] Bass, J., Sharma, A., Wei, Z., Tsoi, M., "Studies of Effects of Current on Exchange-Bias: A Brief Review," *J. of Magnetism (Korean Magnetic Society)* 13, 1 (2008).
- [12] Meiklejohn, W. H., Bean, C. P., "New magnetic anisotropy," *Phys. Rev.* 102, 1413-1414 (1956).
- [13] Nogués, J., Schuller, I. K., "Exchange bias," *J. Magn. Magn. Mater.* 192, 203-232 (1999).
- [14] Berkowitz, A. E., Takano, K., "Exchange anisotropy-a review," *J. Magn. Magn. Mater.* 200, 552-570 (1999).
- [15] Ohldag, H., et al., "Correlation between Exchange Bias and Pinned Interfacial Spins," *Phys. Rev. Lett.* 91, 017203 (2003).
- [16] Scholl, A., Liberati, M., Arenholz, E., Ohldag, H., Stöhr, J., "Creation of an Antiferromagnetic Exchange Spring," *Phys. Rev. Lett.* 92, 247201 (2004).
- [17] Stöhr, J., Siegmann, H. C., [Magnetism: from fundamentals to nanoscale dynamics], Springer Series in Solid-State Sciences, Vol. 152, Springer (2006).
- [18] Slaughter, J. M., Pratt, Jr., W. P., Schroeder, P. A., "Fabrication of layered metallic systems for perpendicular resistance measurements," *Rev. Sci. Instrum.* 60, 127-131 (1989).
- [19] Pratt, W.P., Jr., et al., "Perpendicular-current transport in exchange-biased spin-valves," *IEEE Trans. On Magn.* 33, 3505-3510 (1997).
- [20] Reilly, A. C., et al., "Perpendicular giant magnetoresistance of  $\text{Co}_{91}\text{Fe}_9/\text{Cu}$  exchange-biased spin-valves: further evidence for a unified picture," *J. Magn. Magn. Mat.* 195, L269-L274 (1999).
- [21] Xu, Y., Wang, S., Xia, K., "Spin-transfer torques in antiferromagnetic metals from first principles," *Phys. Rev. Lett.* 100, 226602 (2008).
- [22] Gomonay, H., V. Loktev, V., "Spin-polarized Current-induced Instability in Spin-Valve with Antiferromagnetic Layer," arXiv: 0709.4172.